# Photodegradation of brominated flame retardants in polystyrene: Quantum yields, products and influencing factors

Amina Khaled, Claire Richard, Agnès Rivaton, Farouk Jaber, Mohamad Sleiman

# Photodegradation of brominated flame retardants in polystyrene: quantum yields, products and influencing factors

Amina Khaled[1], Claire Richard[1], Agnès Rivaton[1], Farouk Jaber[2], Mohamad Sleiman[1*]

[1] Université Clermont Auvergne, CNRS, SIGMA Clermont, Institut de Chimie de Clermont-Ferrand, F-63000 Clermont–Ferrand, France.

[2] Laboratory of Analysis of Organic Compounds (509), Faculty of Sciences I, Lebanese University, Hadath, Beirut, Lebanon.

*Corresponding author: M Sleiman

Email: mohamad.sleiman@sigma-clermont.fr

Tel: +33 (0)4 73 40 76 35

**Abstract**

Brominated flame retardants (BFRs) are widely used as additives in plastics, textiles and electronics materials. Here, we investigated the photodegradation of four BFRs including decabromobiphenylether (BDE-209), tetrabromobipsphenol A (TBBPA), tetrabromobisphenol A-bis(2,3-dibromopropylether) (TBBPA-DBPE) and tetrabromobisphenol A bis (allyl) ether (TBBPA-BAE). Experiments were carried out in polystyrene (PS) films using monochromatic and polychromatic irradiations. For comparison, irradiations were also carried in a solvent (tetrahydrofuran: THF). Monitoring of BFR degradation was performed using bulk and surface infrared (IR) measurements, as well as by extraction and HPLC-UV. Photoproducts were characterized using HPLC-high resolution electrospray ionization mass spectrometry (HPLC-ESI-Orbitrap-MS).

All four BFRs underwent photochemical transformation in THF at 290 nm with a quantum yield (Φ) ranging from 0.05 for TBBPA to 0.27 for BDE-209, indicating an increase of photoreactivity with the number of Br atoms in BFRs. On the other hand, no major difference in the Φ values was observed when BFRs were embedded in PS films (Φ: 0.82 - 0.89). The higher photoreactivity in PS appears to be associated with a fast oxidation of PS as revealed by infrared (IR) analysis and yellowing of the films. Interestingly, the faster the yellowing occurred, the faster the BFR degradation was inhibited due to light screening effect. Several major photoproducts were identified for TBBPA and TBBPA-DBPE. Additional photoproducts possibly arising from PS oxidation and bromination by $Br^{\bullet}$ were observed for the first time. This work provides a better understanding of the reactivity and fate of BFRs in polymers allowing for a better assessment of their environmental impacts.

**Keywords:** polybrominated diphenyl ethers, tetrabromobipsphenol A, kinetic, fate.

## 1. Introduction

Brominated flame retardants (BFRs) are ubiquitous industrial chemicals that are commonly used in plastics, textiles and electrical /electronic equipment to improve their fire resistance (de Wit, 2002; Birnbaum and Staskal, 2004). BFRs include more than 75 different substances which belong to three main groups: polybrominated diphenyl ethers and biphenyls (PBDEs and PBBs), hexabromocyclododecanes (HBCDs), tetrabromobisphenol A (TBBPA) and derivates (Alaee et al., 2003). Due to their toxicity and environmental persistence, strict bans on the production and use of several PBDEs (penta-, octa-, deca-BDE) have been introduced. Furthermore, these BFRs were listed under the Stockholm convention for persistent organic pollutants (POPs)(Sindiku et al., 2015). Other emerging BFRs, dubbed as novel BFRs (NBFRs) have been introduced into the market as alternatives to banned formulations. Some of the commonly used NBFRs include decabromodiphenyl ethane or 1,2-bis(pentabromodiphenyl)ethane (DBDPE), 1,2-bis(2,4,6-tribromophenoxy)ethane (BTBPE), 2-ethylhexyl-2,3,4,5-tetrabromobenzoate (TBB or EHTBB), bis(2-ethylhexyl)-3,4,5,6-tetrabromo-phthalate (TBPH or BEHTBP), tetrabromobisphenol A-bis(2,3-dibromopropylether) (TBBPA-DBPE) and tetrabromobisphenol A bis (allyl) ether (TBBPA-BAE). At present, the most widely used BFR is TBBPA (50% of BFRs currently used) with an estimated annual production volume of 130.000 tons (Han et al., 2016). TBBPA-containing materials are used in the manufacturing of office and home electronic equipment, such as computer printed circuit boards, mobile phones, televisions, washing machines, etc. Due to its extensive use, environmental contamination of TBBPA has been detected in various matrices such as air, water, dust and sediments (Morris et al., 2004; Abdallah et al., 2008; Lin, 2015). Moreover, it has been found in exposed humans and animals and was reported to be neurotoxic

and endocrine disruptor (Jakobsson et al., 2002; Cariou et al., 2008; Van der Ven et al., 2008; Geens et al., 2009; Dourson, 2015; Liu et al., 2016; Gong et al., 2017; Inthavong et al., 2017). Various studies have investigated the transformation pathways of TBBPA in the environment, in particularly photodegradation in surface water (Eriksson et al., 2004b; Wang et al., 2015b; Han et al., 2016). Direct photolysis of TBBPA under solar irradiation was found to occur in aqueous solution and via photosensitized reactions with $OH^{\bullet}$ radicals and singlet oxygen generated by irradiation of humic substances (Eriksson et al., 2004b; Han et al., 2009; Wang et al., 2015b; Han et al., 2016). The major phototransformation pathways included debromination and oxidation (Eriksson et al., 2004b; Wang et al., 2015b; Han et al., 2016). While these studies shed light on the photoreactivity of TBBPA in water, no data is available to date on the kinetics and photoproducts of TBBPA in solid polymer matrices as well as on the photodegradation of some of its NBFR derivatives (TBBPA-DBPE and TBBPA-BAE). This is of great significance since TBBPA and its NBFRs derivatives are incorporated in plastics, and absorb solar radiation (>290 nm) which can induce their degradation during use, recycling in landfills or in microplastics contaminating rivers and oceans (Ballesteros-Gómez et al., 2017). As an example, we have recently demonstrated that BDE-209 can undergo photodegradation in car seat fabrics collected from end of life vehicles, leading to the formation of dibenzofurans and dioxins as well as leachates to air and water (Khaled et al., 2018). In this study, our aim was to investigate the photoreactivity of TBBPA and two of its NBFR derivatives (TBBPA-DBPE and TBBPA-BAE) illustrated in Fig. 1. Experiments were performed in tetrahydrofuran (THF) and in PS films. THF was selected due to the high solubility of BFRs in this solvent and its relative stability under UV irradiation. While not all selected BFRs are used in PS materials, we used

it as a model target plastic material due to its wide use and ease of preparation and analysis. In addition to TBBPA NBFR derivatives, BDE-209 was included in the present study as a reference BFR for comparison. This is the first study to examine photodegradation of TBBPA and its NBFR derivatives in solid matrices. The results will help to better assess the environmental fate and impact of these BFRs.

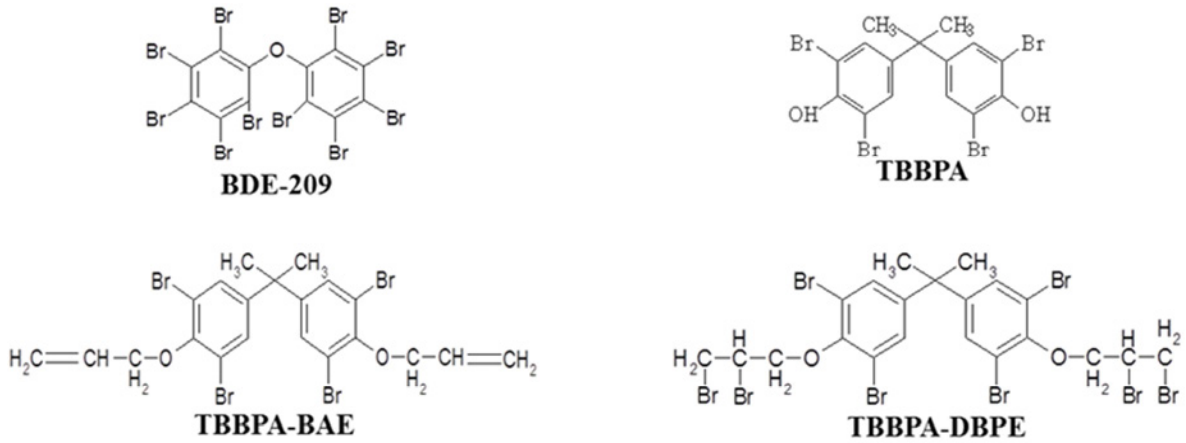


**Fig. 1.**Structures of studied brominated flame retardants (BFRs).

## 2. Materials and Methods

### *2.1. Materials*

Bis (pentabromophenyl) ether (BDE-209, 98% purity) was purchased from Sigma Aldrich, Germany. The three other flame retardants standards such as Tetrabromobisphenol A (TBBPA, >98% purity), 2.2-Bis [3.5-dibromo-4-(2.3-dibromopropoxy) phenyl] propane (TBBPA-DBPE >90% purity), and 2.2-Bis (4-allyloxy-3.5-dibromophenyl) propane (TBBPA-BAE>99% purity) were obtained from Tokyo Chemical Industry (TCI Europe, Belgium). THF and acetonitrile (ACN) were of HPLC grade purity (99%) and obtained from Sigma-Aldrich, Germany. The studied polymer was PS material without additive (Mw=172175 g $mol^{-1}$) in powder form.

*2.2. Samples preparation*

**- In THF.** The solutions of BDE-209, TBBPA, TBBPA-DBPE and TBBPA-BAE were prepared at a concentration of $10^{-4}$ M. All solutions were stored in the dark at room temperature.

**- PS film preparation**. It is important to note that the TBBPA-BAE molecule has not been studied in PS because of the difficulties of preparing PS films containing TBBPA-BAE by extrusion at high temperature. The two other brominated additives (TBBPA and TBBPA-DBPE) in an amount of 2% in weight were incorporated into the PS matrix by an extrusion process, using a Haake Minilab twin-screw extruder device. Laboratory experimental conditions were: T=180 ℃, with a roller speed of 100 rpm for 5 min. Then films of PS and PS/BFRs (approximately ≈80-85 µm thickness) were prepared by compression molding between PTFE-coated glass cloths at 200 bars in an electrically heated laboratory press at 180 ℃ for 3 min.

*2.3. Extraction of BFRs from PS*

The BFRs contents in polystyrene samples were extracted and quantified as follows: 0.01g of PS films was dissolved into 2ml THF then mixed by vortex for 1min. Then, 1ml of the extracts was centrifuged for 5 min at 13500 rpm before analysis. Before irradiation, the recovery efficiency (95±5%) of the extraction procedure was evaluated by the analysis of three blank PS samples spiked with known amounts of BFRs.

*2.4. Irradiations*

To determine quantum yield of BFRs, solutions were irradiated in a quartz cuvette in a parallel beam using a high pressure mercury arc lamp equipped with an oriel monochromator with a wavelength (λ) fixed at 290nm for all irradiations experiments

in THF. The quartz cuvette was hermetically closed by a stopper to avoid THF losses by evaporation. All photodegradation experiments were performed in triplicate. The different irradiation parameters are given in Table 1A. For PS/BFR films, irradiation was carried out using the same irradiation system cited above (monochromator). The different irradiation parameters are given in Table 1.B. The initial and remaining BFRs concentrations in PS films were determined by HPLC analysis after extraction by THF (as described later in section 2.5.2).

The quantum yield values were the average of two independent measurements. The quantum yields (Φ) of photodegradation were calculated based on the following equations:

$$\emptyset = \frac{\Delta n}{\overline{I_a} \times \Delta t}$$

where Δn is the number of photodegraded molecules during Δt, the irradiation time, and $\overline{I_a}$, the average number of absorbed photons during the irradiation time ($\Delta t$).

- In THF: Δn=Δc x N where Δc is the concentration decrease expressed in mole/cm$^3$ measured by HPLC and N the Avogadro number, $\overline{I_a} = \frac{I_a^{t0} + I_a^t}{2}$, where $I_a^{t0} = \frac{Io}{\ell}\left(1 - 10^{-A_{BFR}^{t0}\lambda}\right)$ and $I_a^t = \frac{Io}{\ell}\left(1 - 10^{-A_{BFR}^{t}\lambda}\right)$, where $I_o$ is the photon flux expressed in photon/cm$^2$/s, $A_{BFR}^{t0}\lambda$ the initial absorption at wavelength λ of BFR, $A_{BFR}^{t}\lambda$ the absorbance of BFR at instant t after irradiation, and ℓ, the path length (1cm) . The contribution of THF to the absorbance of the solution is negligible at the irradiation wavelength (290 nm).
- In PS: Δn is obtained by multiplying $n_o$, the initial number of molecules in the sample by the percentage of degradation measured by HPLC. $n_o$ was calculated using the volume of the sample (0.0083 cm$^3$), a density of 1g cm$^{-3}$

and a loading of 2% in weight. Since PS can also contribute to the absorbance of the film PS/BFR, we used the following expressions to calculate $I_a^{t0}$ and $I_a^t$: $I_a^{t0} = \frac{Io}{\ell}\left(1 - 10^{-A_{BFR}^{t0}\lambda}\right)$ where $I_o$ is the photon flux expressed in photon/cm$^2$/s, $\ell$ is the film thickness (80-85 µm) and $A_{BFR}^{t0}\lambda$ is the initial absorbance of BFR (at 2% in weight) in the PS film (for a path length $\ell$) corrected by subtracting the contribution of PS initial absorbance at the same λ which was negligible at the selected λ for irradiating the PS/BFR films (as shown later in section 3.1, Figure 2). After irradiation, the contribution of PS to the total absorbance increased due to yellowing (as described later in the results section) and thus a correction of the measured absorbance was performed as follows: $I_a^t = \frac{Io}{\ell} * \frac{A_{BFR}^t}{A_{PS+BFR}^t}\left(1 - 10^{-A_{BFR}^t\lambda}\right)$, where $A_{PS+BFR}^t$ represents the total absorbance of irradiated PS/BFR film and $A_{BFR}^t$ is the absorbance of BFR in the PS film after irradiation, as estimated by multiplying the initial absorbance $A_{BFR}^{t0}$ by the percentage of remaining BFR in the PS film after irradiation (by extracting and analyzing BFR using HPLC as described later in section 2.5.2).

For the purpose of photoproducts identification, irradiation of films was carried out using a Suntest CPS photosimulator from Atlas equipped with a Xenon arc lamp and a special glass filter that restricted the transmission of wavelengths below 290 nm. The irradiance was set at 500 Wm$^{-2}$, whereas the emitted wavelengths ranged from 290 to 800 nm. The temperature within the dishes did not exceed 25 ℃ thanks to a water circulation cooling system maintained at 10 °C. Irradiation of the samples in THF was carried out using a polychromatic device equipped with six fluorescent tubes TLAD 15W05 Philips (300-450 nm, emission maximum at 365 nm) at room temperature. A 20 ml capacity Pyrex-glass cylindrical reactor (1.4 cm, i.d.) was used

and closed with a stopper to avoid THF evaporation. For all photolysis experiments, duplicate samples were irradiated.

### *2.5. Analytical methods*

#### *2.5.1. Spectroscopic Analyses*

Absorption spectra of BFRs solutions in THF were recorded using a Cary 3 UV-Visible spectrometer (Varian) in a quartz cuvette. Solid state UV-Visible spectra were obtained with a UV2600 spectrophotometer equipped with an integrating sphere from Shimadzu. Infrared (IR) spectra of PS films were recorded in transmission mode using a Nicolet 760-FTIR spectrophotometer (nominal resolution of $4cm^{-1}$, 32 scan summations), and also in reflection mode with a Nicolet 380-FTIR spectrophotometer equipped with a Thunderdome-ATR accessory with a diamond crystal (4 $cm^{-1}$, 32 scans). Note that unlike Transmission IR spectroscopy which probes the entire thickness of the material, ATR-IR technique generates only a few microns depth penetration of the IR beam in the sample thickness. Therefore it is commonly considered that IR spectrum obtained using a diamond ATR crystal provides information regarding the first 3–5 µm superficial layer of solid materials. All absorbance values presented are an average of at least four samples.

#### *2.5.2. HPLC Analysis*

All BFRs samples in THF and in PS were analysed using a Shimadzu liquid chromatography type equipped with a UV-visible absorption detector SPD-M20A. A 10 µl aliquot was injected in a Marchery-Nagel Nucleodur column $C_8$ grafted silica of 250 mm length and of 4.6 of particle mm i.d, at a flow rate of 1ml $min^{-1}$ and the mobile phase consisted of 100% ACN for BDE-209, TBBPA-DBPE, and 80% ACN-20% water for TBBPA. The peaks for each compound were identified in the chromatogram

by comparing the retention times of the analyte in the liquid sample and in the PS. Photoproducts in THF and PS were identified using an HP 3000 RSLC high performance liquid chromatography system (ThermoScientific) equipped with a high resolution Orbitrap mass spectrometry analyzer. Samples were injected onto a Kinetex™ $C_{18}$ LC column (100 mm × 2.1 mm, 1.7 µm particle sizes). The binary solvent system used was composed of ACN and water acidified with 0.5‰ v/v formic acid. The gradient program was 5% ACN for the 7 first min, followed by a linear gradient to 99% in 7.5min and kept constant until 20 min. The flow rate was set at 0.45 mL $min^{-1}$ and injection volume was 5 µL. Scan parameters were set from m/z 120 to 1800 amu in full-scan negative ESI ionization mode. To identify unknown photoproducts, the mass accuracy was set at <5 ppm. Chemical structures are proposed based on the mass spectra and bromine isotope patterns

## 3. Results and discussion

### *3.1. UV-Vis absorption spectra*

The absorption spectra of the studied BFRS in THF are presented in Fig. 2A. Compared to BDE-209, TBBPA derivatives absorb at shorter wavelength. TBBPA shows an absorption band extending from 260 to 310 with two maxima at 283-293nm. TBBPA-DBPE and TBBPA-BAE have similar absorption band, but much less intense than TBBPA and shifted to the blue by about 10 nm. Thus, one can assume that the addition of side groups to the TBBPA moiety in TBBPA-DBPE and TBBPA-BAE reduces light absorption and could thus help to reduce photodegradation. Nevertheless, the band edges around 300 nm make possible solar photons absorption ($\lambda$ > 290 nm). The absorption of BFRs above 300 nm is more obvious in the PS samples loaded at 2% in weight (Fig. 2B).

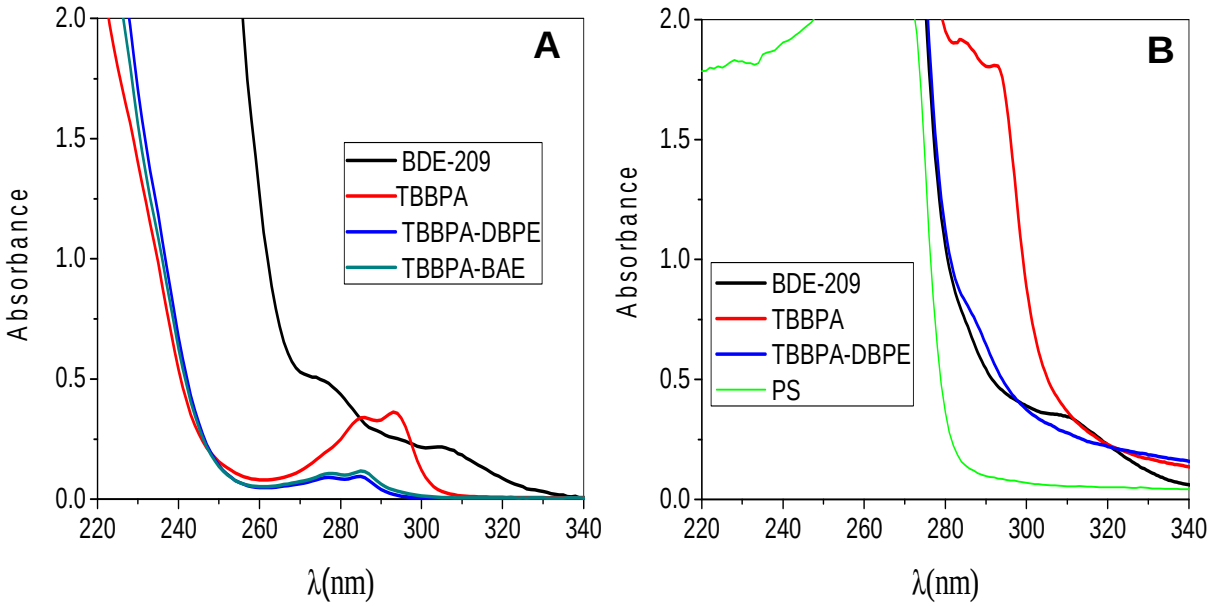


209 **Fig. 2. (A)** UV-vis absorption spectra of BFRs in THF; **(B)** UV-vis absorption spectra
210 of BFRs (2% w:w) in PS.

211 This suggests that photodegradation of incorporated BFRs could take place during
212 UV exposure of PS. The 2% loading was selected because it is comparable to BFRs
213 concentration used in polymers (2-20%) while avoiding to reach absorbance
214 saturation at high percentage. Since PS can absorb light <280nm as shown in Fig.
215 2B, we choose to irradiate BFRs at higher wavelengths (λ >290nm) to avoid
216 screening effect due to PS light absorption and to mimic solar light.

217 *3.2. Quantum yields of photodegradation*

218 Dark control experiments for each BFR did not show any noticeable degradation
219 (<2%). The quantum yields of BFRs degradation in THF upon monochromatic
220 excitation at 290nm are presented in Table 1A.

Φ values ranged between 0.05 for TBBPA and 0.27 for BDE-209. TBBPA-DBPE (0.190) and TBBPA-BAE (0.08) exhibited in-between values. These values are close to those reported for BDE-209 in water (0.28) and in THF (0.38), and for TBBPA

(0.018-0.045) in water depending on pH values (Eriksson et al., 2004b; Kuivikko et al., 2007; Xie et al., 2009). However, this is the first time that quantum yield of photodegradation is reported for TBBPA-DBPE and TBBPA-BAE.

**Table 1A.** Quantum yields (Φ) of BFRs ($10^{-4}$ M) in THF.

| BFR | Concentration (M) | Absorbance at 290 nm | Time (min) | loss (%) | $I_0$(photon/cm$^2$/s) | Φ |
|---|---|---|---|---|---|---|
| BDE-209 | $10^{-4}$ | 0.30 | 5 | 14% | $2.2x10^{14}$ | 0.27±0.03 |
| TBBPA | $10^{-4}$ | 0.64 | 10 | 14% | $3.6x10^{14}$ | 0.05±0.02 |
| TBBPA-DBPE | $10^{-4}$ | 0.11 | 5 | 8% | $3.6x10^{14}$ | 0.19±0.02 |
| TBBPA-BAE | $10^{-4}$ | 0.15 | 30 | 26% | $3.6x10^{14}$ | 0.08±0.01 |

**Table 1B.** Quantum yields (Φ) of BFRs (2% in weight) in PS films (80-85µm)

| BFR | λ nm | $N_0$ (mole/cm$^3$) | Absorbance | Time (h) | loss% | $I_a$(photon/cm$^2$/s) | Φ |
|---|---|---|---|---|---|---|---|
| BDE-209 | 310 | $2.08x10^{-5}$ | 0.29 | 2 | 20% | $3.9x10^{14}$ | 0.89±0.08 |
| TBBPA | 302 | $3.6x10^{-5}$ | 0.29 | 8 | 34% | $3.11x10^{14}$ | 0.82±0.08 |
| TBBPA-DBPE | 285 | $2.1x10^{-5}$ | 0.4 | 7 | 21% | $1.25x10^{14}$ | 0.84±0.08 |

The order of photoreactivity seems to correlate with the number of Br atoms present in the molecules. As an example, TBBPA with 4 Br atoms exhibits the lowest Φ followed by TBBPA-BAE (6Br), TBBPA-BDBPE with 8 Br (Φ = 0.19), whereas for BDE-209 (10 Br) Φ is the highest (0.27).This finding is in agreement with previous studies showing that the higher brominated diphenylethers photodegrade faster than lower brominated (Eriksson et al., 2004a; Fang et al., 2008; Wang et al., 2015a; Staszowska, 2017). Our study reveals that this correlation can be also verified when comparing brominated flame retardants which do not share the same core structure such as TBBPA and BDE-209. On the other hand, the calculated Φ values for the 3

BFRs in PS vary in a very narrow range (0.82 - 0.89) as shown in Table 1B, indicating that the correlation based on the number of Br is not valid in PS. Surprisingly, these values are much higher than those found in THF. In a previous study, we have shown that BDE-209 exhibits very high photoreactivity in PS compared to other polymers such as PET and cellulose (Khaled et al., 2018). While the reasons for this high photoreactivity in PS are not clear, several assumptions can be postulated:

- a higher hydrogen donor capacity of PS which can promote debromination and thus accelerate photodegradation (Kajiwara et al., 2008; Khaled et al., 2018). This can be explained by the lower C-H bond dissociation energy in PS or Ar-C-H (386 kJ/mol) than in THF (410 kJ/mol) (Agapito et al., 2005). This lower dissociation energy in PS can facilitate the debromination via formation of HBr.

- π- π stacking between PS and BFRs (Pan et al., 2013). A recent study has shown via theoretical calculations that face-to-face π- π stacking interaction plays an important role in the low-lying π→σ* transitions of BDE209−toluene π-stacking complex at around 300 nm in the sunlight region. This leads to notable changes for the πσ* excited states and promotes the breaking of the C−Br bonds. The photodegradation reaction via an intermolecular charge-transfer excited state formed by the electronic transition from a π orbital of toluene to a σ* orbital of BDE209 was thus found to be a dominant mechanism. Given the similarity between toluene and styrene, we hypothesize that a similar π- π stacking interaction interaction could occur in PS/BFR resulting in a favorable condition for C-Br photolysis. Further investigations are needed to confirm this assumption.

- an auto-acceleration effect due to mutual interaction between the PS and Br radicals released by the photodegradation of BFRs. It is possible that the first Br radicals released by debromination cause change in PS structure and lead to the formation of reactive species which can in turn enhance the degradability of BFRs.

It is important to note that the Φ values were not calculated at the linear initial stage of the reaction due to the difficulty to measure very low conversion extents. Thus, longer irradiation times (2-8 h of exposure compared to 5-30 min of exposure for THF solution) were required, and secondary reactions (e.g. degradation of primary photoproducts, oxidation of PS, formation of adducts, etc.) may have taken place. In particular, a significant yellowing of the films was observed. This yellowing induces a decrease in $I_a$ during irradiation due to the competition of absorbance between BFRs and PS yellowing byproducts which can affect the Φ measurement. The other possible bias is that BFRs concentration measurements were performed after dissolution of the films in THF. The percentage of conversion obtained is thus an averaged value inside the film sample and it does not reflect the potential heterogeneous BFRs photodegradation inside the films due for instance to an oxidation profile as previously suggested (Torikai et al., 1995; Sinturel et al., 1999). To examine the oxidation profile of BFRs in the PS film, ATR-IR measurements were carried out on both sides of the irradiated film (the first 3-5 µm surface layer) in addition to transmission IR analysis (the whole thickness of the film) before film dissolution and HPLC-UV analysis. The photodegradation occurred more significantly at the irradiated face of the PS film. After 2h of irradiating PS containing BDE-209, the average conversion extent measured by HPLC and IR was around 20% while the measurement by ATR-IR (Fig S1) indicates 33% for the exposed surface (upper) and 23% for the non-exposed surface (lower) as it can be seen in Fig. S1 and Table S2. It

can be concluded that the photodegradation of BFRs is indeed heterogeneous in PS and thus data presented in Table 1B are consequently only indicative and must be taken with care.

### *3.3. Kinetics of BFRs photodegradation*

We measured the decay profiles of BFRs in THF (Fig. 3A) and in the PS films under polychromatic irradiation: between 300-450 nm for THF solutions using a photoreactor and between 300-800 nm for PS films using the SUNTEST device (Fig. 3B). In THF, the rate of BFRs photodegradation varied in the order BDE-209 >> TBPPA >> TBPPA-DBPE. The rate is related to the product $I_a\Phi$. The dominant factor here is likely the light absorption that is much more important for BDE-209 and in a minor extent for TBPPA than for the TBBPA-DBPE (see Fig. 2A).

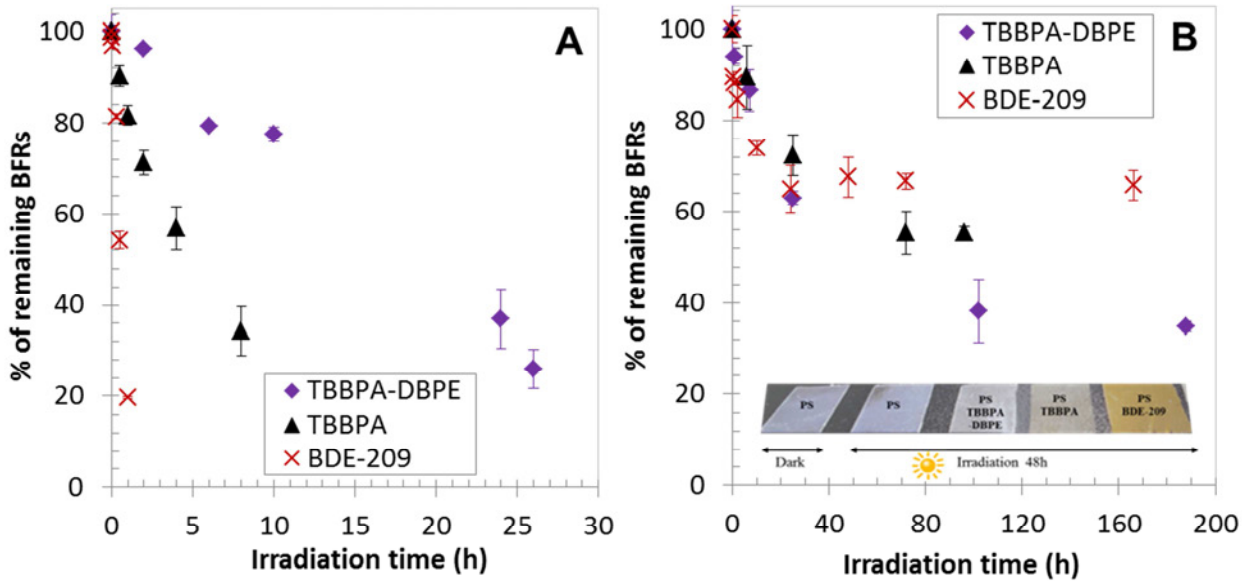


**Fig. 3. (A)** Decay profiles of BFRs ($10^{-4}$ M) irradiated in THF (300-450 nm). Error bars represent the relative standard deviation obtained from triplicate measurements. **(B)** Decay profiles of BFRs in PS irradiated in the Suntest solar simulator (300-800 nm, 500 W $m^{-2}$).

In PS films, when one considers the early stages of the reactions (the first 10h of exposure), the highest rate of photodegradation is observed for BDE-209, which is due to its high absorption in the range 290-365nm. At higher extent of the reaction (> 40h), differences are observed in the plateau values reached. BDE-209 is the BFR the less photodegraded with a maximum of ~30%. TBPPA reaches 45% of photodegradation, followed by TBPPA-DBPE (62%). This is almost in the opposite order of the rate of photodegradation measured in THF and what is measured during the initial stage of PS films exposure. A plausible explanation is that a low initial rate of BFRs phototransformation induces a low rate of PS degradation, thus a low yellowing (see Fig. 3B inset) and therefore a small impact of the polymer matrix on BFRs photodegradation. On the contrary, a fast rate of BFRs photodegradation results in a fast rate of PS degradation, an intense yellowing (Fig. 3B) and therefore an important inhibiting effect of the degraded polymer matrix on the BFRs photodegradation through a light screening effect. This latter is confirmed by the increase of absorption of PS films at higher wavelengths (> 300 nm) after 24h of irradiation as depicted in Fig. S2 (A,B,C). Consequently, despite a lower light absorption for TBBPA-DBPE than TBBPA, its photodegradation during the lifetime of the polymer will be more extensive than TBBPA. This finding questions the strategy of using less absorbing BFR additives as an efficient solution to avoid or minimize photodegradation. Moreover, it raises the question of the impact of enhanced photodegradation on the long-term efficiency of BFRs and its environmental impacts.

### *3.4. Photoproducts of TBBPA and TBBPA-DBPE in THF and PS*

Tables 2 and 3 summarize the major photoproducts detected during photolysis of TBBPA and TBBPA-DBPE respectively in THF and in PS. To obtain a valid comparison, samples were irradiated for different durations to reach the same level of

conversion in both media at about 45 ± 5%. Due to experimental constraints, the photoproducts of TBBPA-BAE were only identified in THF and are presented in Table S1. Overall, eleven major photoproducts for each BFR were identified, assigned as products A1-A11 for TBBPA photoproducts and B1-B11 for TBBPA-DBPE. To our knowledge this is the first study to report on the products of TBBPA-DBPE and TBBPA-BAE. According to the proposed structures of the photoproducts, products A1 and A2 are formed by debromination of TBBPA, products A3-A5 can result from debromination and replacement of bromine by OH group. With the exception of A5, products A1-A4 were detected in both THF and PS under irradiation. The formation of hydroxyated products of BFRs in PS suggest that oxygen or water vapor present in the air are involved in the photodegradation mechanisms. Moreover, all these products have also been reported in previous studies of TBBPA photolysis in water (Wang et al., 2015b). On the other hand, product A6 appears to be only detected in PS. While it is not clear how A6 might arise from TBBPA, this products is a derivative of benzophenone, a well know photosensitizer , it may therefore contribute to PS oxidation (Lin et al., 1992). A7 has been previously detected during TBBPA photolysis in water (Eriksson et al., 2004a; Eriksson et al., 2004b; Bao and Niu, 2015). It could result from C-C scission, followed by oxidation (Wang et al., 2015b). Further oxidation of A7 could lead to product A8 whereas bromination could lead to tribromophenol (product A9). This latter was commonly detected during TBBPA photolysis (Bao and Niu, 2015; Wang et al., 2015b). Products A10-A11 are only observed in PS and thus are likely to be generated by oxidation of PS and bromination by released $Br^{\bullet}$ radicals. This suggests a new mechanism of degradation of polymers containing BFRs.

343 **Table 2.** Identified TBBPA photoproducts at 45±5% degradation in THF and in PS. *THF, $^{+}$PS. $^{a}$Only the monoisotopic and most intense m/z are
344 presented.

| Chemical formula | m/z[a] | Structure |
|---|---|---|
| **A1- $C_{15}H_{13}O_2Br_3^{*+}$**<br>**$C_{15}H_{13}O_2\ ^{79}Br_2\ ^{81}Br$** | 460.8396<br>462.8374 | 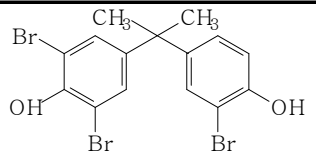 |
| **A2- $C_{15}H_{14}O_2Br_2^{*+}$**<br>**$C_{15}H_{14}O_2\ ^{79}Br\ ^{81}Br$** | 382.9289<br>384.9268 | 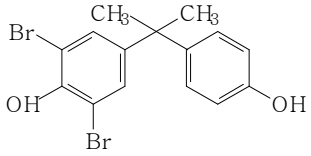 |
| **A3- $C_{15}H_{13}O_3Br_3^{*+}$**<br>**$C_{15}H_{14}O_3\ ^{79}Br_2\ ^{81}Br$** | 476.8344<br>478.8321 | 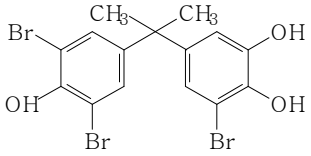 |
| **A4- $C_{15}H_{14}O_3Br_2^{*+}$**<br>**$C_{15}H_{14}O_3\ ^{79}Br\ ^{81}Br$** | 398.9237<br>400.9217 | 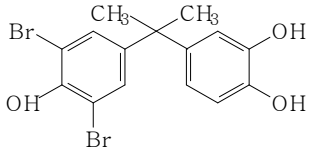 |
| **A5- $C_{15}H_{14}O_4Br_2^{*}$**<br>**$C_{15}H_{14}O_4\ ^{79}Br\ ^{81}Br$** | 414.9189<br>416.9167 | 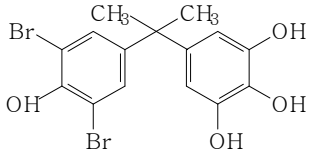 |
| **A6- $C_{13}H_6O_3Br_4^{+}$**<br>**$C_{13}H_6O_3\ ^{79}Br_2\ ^{81}Br_2$** | 528.6942<br>526.6965 | 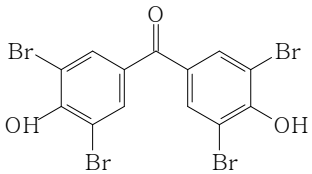 |
| **A7- $C_9H_{10}O_2Br_2^{*+}$**<br>**$C_9H_{10}O_2\ ^{79}Br\ ^{81}Br$** | 306.8975<br>308.8955 | 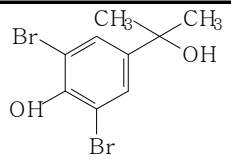 |
| **A8- $C_9H_{10}O_3Br_2^{*+}$**<br>**$C_9H_{10}O_3\ ^{79}Br\ ^{81}Br$** | 322.8928<br>324.8904 | 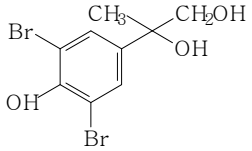 |
| **A9- $C_7H_4O_3Br_2^{+}$**<br>**$C_7H_4O_3\ ^{79}Br\ ^{81}Br$** | 294.8434<br>294.8457 | 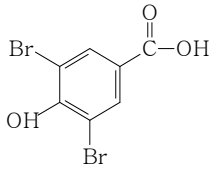 |
| **A10- $C_7H_5O_2Br^{+}$** | 198.9392<br>200.9372 | 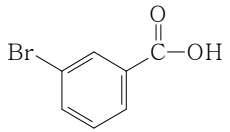 |
| **A11- $C_6H_3OBr_3^{*+}$**<br>**$C_6H_3O\ ^{79}Br_2\ ^{81}Br$** | 326.7661<br>328.7641 | 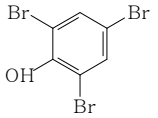 |

345 **Table 3.** Identified TBBPA-DBPE photoproducts at (45±5%) degradation in THF and in PS. *THF, $^{+}$PS. $^{a}$Only the monoisotopic and most
346 intense m/z are presented.

| Chemical formula | m/z | Structure |
|---|---|---|
| **B1- $C_{21}H_{21}O_3Br_7^{*+}$**<br>**$C_{21}H_{21}O_3\,^{79}Br_3\,^{81}Br_4$** | 874.5690<br>878.5642 | 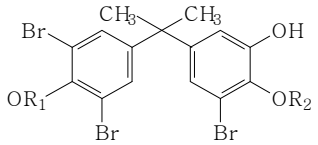 |
| **B2- $C_{18}H_{16}O_2Br_6^{*+}$**<br>**$C_{18}H_{16}O_2\,^{79}Br_3\,^{81}Br_3$** | 738.6168<br>742.6127 | 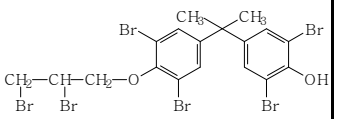 |
| **B3- $C_{18}H_{17}O_3Br_5^{*+}$**<br>**$C_{18}H_{17}O_{43}\,^{79}Br_3\,^{81}Br_2$** | 676.6995<br>678.6975 | 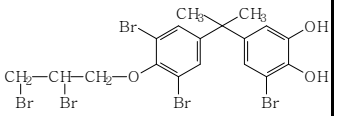 |
| **B4- $C_{18}H_{16}O_2Br_4^{*+}$**<br>**$C_{18}H_{16}O_2\,^{79}Br_2\,^{81}Br_2$** | 578.7817<br>582.7773 | 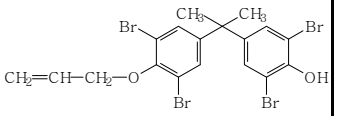 |
| **B5- $C_{18}H_{17}O_2Br_3^{*+}$**<br>**$C_{18}H_{17}O_2\,^{79}Br_2\,^{81}Br$** | 500.8712<br>502.8691 | 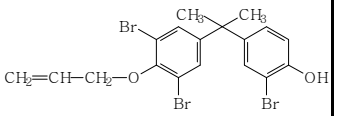 |
| **B6- $C_{15}H_{12}O_2Br_4^{*+}$**<br>**$C_{15}H_{12}O_2\,^{79}Br_2\,^{81}Br_2$** | 538.7503<br>542.7459 | 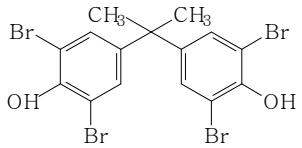 |
| **B7- $C_{15}H_{13}O_2Br_3^{*+}$**<br>**$C_{15}H_{13}O_2\,^{79}Br_2\,^{81}Br$** | 460.8398<br>462.8377 | 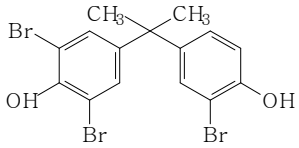 |
| **B8- $C_7H_5O_3Br^{+}$** | 216.9322<br>214.9342 | 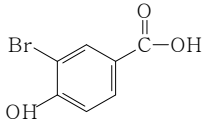 |
| **B9- $C_7H_4O_3Br_2^{+}$**<br>**$C_7H_4O_3\,^{79}Br\,^{81}Br$** | 294.8434<br>294.8457 | 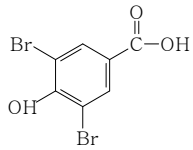 |
| **B10- $C_7H_5O_2Br^{+}$** | 198.9392<br>200.9372 | 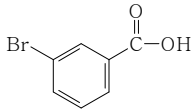 |
| **B11- $C_6H_3OBr_3^{*+}$**<br>**$C_6H_3O\,^{79}Br_2\,^{81}Br$** | 326.7661<br>328.7641 | 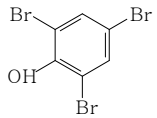 |

For TBBPA-DBPE, the primary intermediates arose from debromination followed by oxidation of the phenyl side to yield the hydroxylated product (B1) and ether bond cleavage (B2). The formation of these products can occur in the presence of water as shown in Scheme 1. The mechanism of debromination on the phenyl side was previously reported during photodegradation of NBFRs such as DPTE (2.3-dibromopropyl-2-4-6-tribromophenylether)(Zhang et al., 2016). These intermediates can further degrade to produce photoroducts B3 and B4. B3 could arise from ether bond cleavage of B1 whereas B4 might be formed by successive debromination and H-abstraction on the alkyl side of B2 yielding a C=C double bond in B4(Liu et al., 2017). A subsequent degradation of B4 through debromination on the phenyl moiety could lead to the formation of B5 or to the generation of B6 (TBBPA) via ether bond cleavage. Other studies have also found that TBBPA can be a major photoproduct of NBFR derivatives of TBBPA (Qu et al., 2013; Liu et al., 2017). The remaining photoproducts (B7-B11) are similar to those found during TBBPA photodegradation, as discussed above. These photoproducts belong to the group of bromophenols and bromobenzoic acid derivatives. In a previous study, we have demonstrated the potential transfer of bromophenols from solid polymeric matrices to water. Hence, further investigation should be performed to assess the toxicity and risk of these photoproducts in water. While the main reaction pathways for TBBPA and TBBPA-DBPE appear to be similar, a competition can occur initially between the reactivity of the brominated side groups (OR1 and OR2) via ether cleavage and the debromination of the tetrabromobisphenol moiety. This competition can reduce the extent of debromination initially as compared to TBBPA and thus a less pronounced bromination and oxidation of PS by released Br. This seems to be consistent with the lower yellowing of PS film observed when TBBPA is replaced by TBBPA-DBPE.

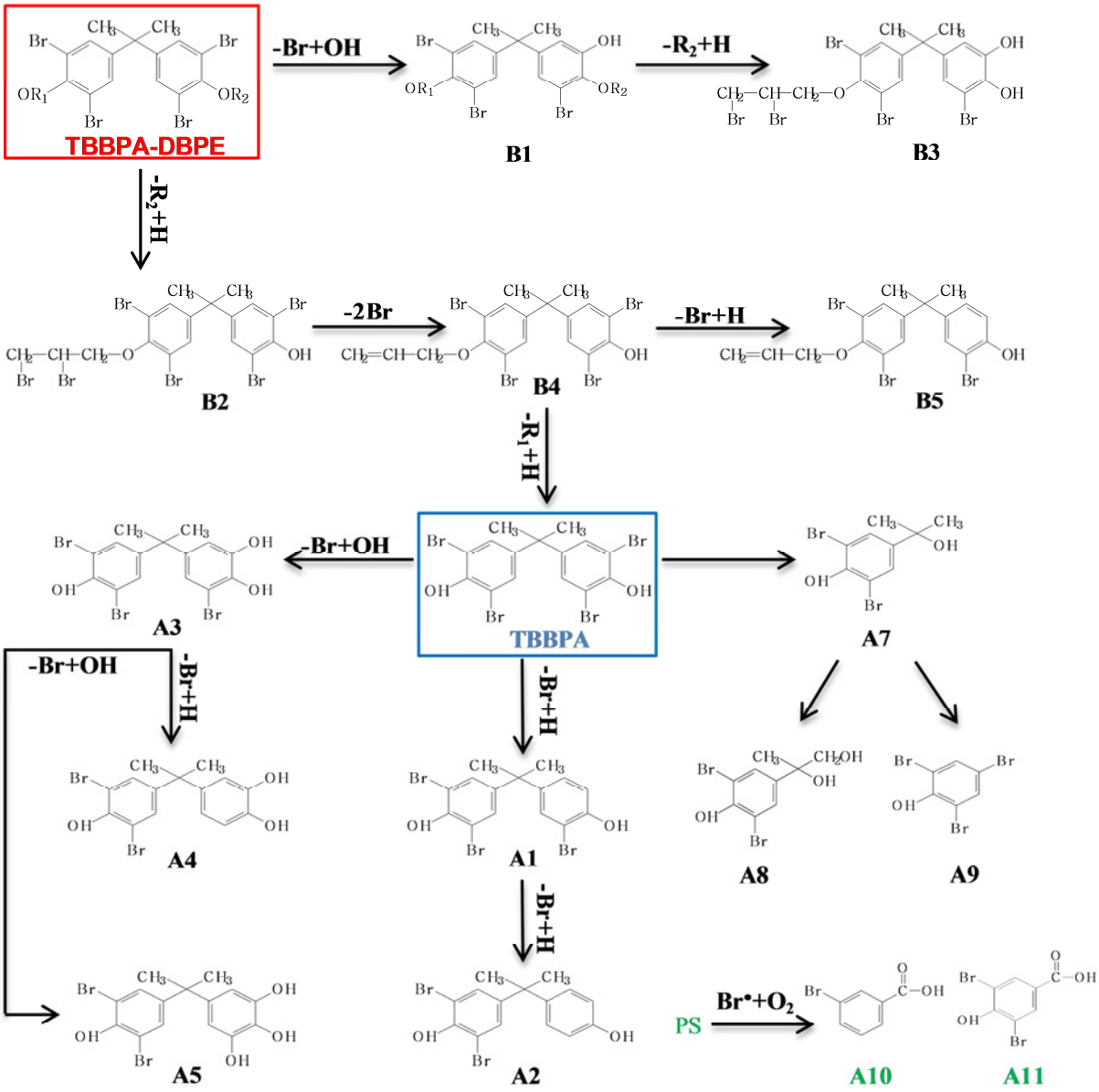


372 **Scheme 1.** Proposed TBBPA and TBBPA-DBPE photodegradation pathways in
373 polystyrene (PS).

374 **4. Conclusion**

375 In this study, quantum yields of BFRs photodegradation were determined in solution
376 (THF) and in polymer (PS) under monochromatic irradiation. Overall, higher values of
377 Φ were obtained in PS than in THF and a significant yellowing of the irradiated PS
378 film was observed. This shows the existence of a mutual accelerating effect. At

longer irradiation duration in a solar simulator, the yellowing of PS was found to inhibit BFRs photodegradation via light screening effect, leading to a stationary state within 2-3 days of irradiation. Interestingly, the higher the initial absorbance of BFR above 290 nm, the fastest it degrades initially, causing a yellowing of the PS film which in turn inhibits BFR from being further degraded.

Analysis of TBBPA and TBBPA derivatives showed similar photoproducts in PS and in THF. Nonetheless, some photoproducts, potentially brominated C7 derivatives were only detected in PS, these products might be resulting from PS oxidation. In addition, new BFR photoproducts never reported in the literature were identified for the first time, thus allowing to complete the mechanisms of their photodegradation. Further, investigation should be performed to better understand the mechanism of PS oxidation in the presence of BFRs. Moreover, assessments of environmental exposure and the resulting health impacts of the transformation products of TBBPA derivatives warrant further study.

## Acknowledgments

Amina Khaled thank the embassy of France in Lebanon for financial support through the fellowship SAFAR and the Lebanese Association for Scientific Research (LASeR) for its financial support. The authors thank Martin Leremboure for helping in the identification of photoproducts using the LC-ESI-orbitrap mass spectrometry. We also thank Guillaume Voyard for his technical help with the maintenance of the HPLC.

## References

Abdallah, M.A., Harrad, S., Covaci, A., 2008. Hexabromocyclododecanes and tetrabromobisphenol-A in indoor air and dust in Birmingham, U.K: implications for human exposure. Environ Sci Technol 42, 6855-6861.

Agapito, F., Cabral, B.J.C., Simões, J.A.M., 2005. Carbon–hydrogen bond dissociation enthalpies in ethers: a theoretical study. Journal of Molecular Structure: THEOCHEM 719, 109-114.

Alaee, M., Arias, P., Sjödin, A., Bergman, Å., 2003. An overview of commercially used brominated flame retardants, their applications, their use patterns in different countries/regions and possible modes of release. Environment International 29, 683-689.

Ballesteros-Gómez, A., Ballesteros, J., Ortiz, X., Jonker, W., Helmus, R., Jobst, K.J., Parsons, J.R., Reiner, E.J., 2017. Identification of Novel Brominated Compounds in Flame Retarded Plastics Containing TBBPA by Combining Isotope Pattern and Mass Defect Cluster Analysis. Environmental Science & Technology 51, 1518-1526.

Bao, Y., Niu, J., 2015. Photochemical transformation of tetrabromobisphenol A under simulated sunlight irradiation: Kinetics, mechanism and influencing factors. Chemosphere 134, 550-556.

Birnbaum, L.S., Staskal, D.F., 2004. Brominated flame retardants: cause for concern? Environ Health Perspect 112, 9-17.

Cariou, R., Antignac, J.P., Zalko, D., Berrebi, A., Cravedi, J.P., Maume, D., Marchand, P., Monteau, F., Riu, A., Andre, F., Le Bizec, B., 2008. Exposure assessment of French women and their newborns to tetrabromobisphenol-A: occurrence measurements in maternal adipose tissue, serum, breast milk and cord serum. Chemosphere 73, 1036-1041.

de Wit, C.A., 2002. An overview of brominated flame retardants in the environment. Chemosphere 46, 583-624.

Dourson, R.B.C.a.K.b.M., 2015. A reproductive, developmental and neurobehavioral study following oral exposure of tetrabromobisphenol A on Sprague-Dawley rats. 329.

Eriksson, J., Green, N., Marsh, G., Bergman, A., 2004a. Photochemical decomposition of 15 polybrominated diphenyl ether congeners in methanol/water. Environ Sci Technol 38, 3119-3125.

Eriksson, J., Rahm, S., Green, N., Bergman, A., Jakobsson, E., 2004b. Photochemical transformations of tetrabromobisphenol A and related phenols in water. Chemosphere 54, 117-126.

Fang, L., Huang, J., Yu, G., Wang, L., 2008. Photochemical degradation of six polybrominated diphenyl ether congeners under ultraviolet irradiation in hexane. Chemosphere 71, 258-267.

Geens, T., Roosens, L., Neels, H., Covaci, A., 2009. Assessment of human exposure to Bisphenol-A, Triclosan and Tetrabromobisphenol-A through indoor dust intake in Belgium. Chemosphere 76, 755-760.

Gong, W.J., Zhu, L.Y., Jiang, T.T., Han, C., 2017. The occurrence and spatial-temporal distribution of tetrabromobisphenol A in the coastal intertidal zone of Qingdao in China, with a focus on toxicity assessment by biological monitoring. Chemosphere 185, 462-467.

Han, S.K., Sik, R.H., Motten, A.G., Chignell, C.F., Bilski, P.J., 2009. Photosensitized oxidation of tetrabromobisphenol a by humic acid in aqueous solution. Photochem Photobiol 85, 1299-1305.

Han, S.K., Yamasaki, T., Yamada, K., 2016. Photodecomposition of tetrabromobisphenol A in aqueous humic acid suspension by irradiation with light of various wavelengths. Chemosphere 147, 124-130.

Inthavong, C., Hommet, F., Bordet, F., Rigourd, V., Guerin, T., Dragacci, S., 2017. Simultaneous liquid chromatography-tandem mass spectrometry analysis of brominated flame retardants (tetrabromobisphenol A and hexabromocyclododecane diastereoisomers) in French breast milk. Chemosphere 186, 762-769.

Jakobsson, K., Thuresson, K., Rylander, L., Sjodin, A., Hagmar, L., Bergman, A., 2002. Exposure to polybrominated diphenyl ethers and tetrabromobisphenol A among computer technicians. Chemosphere 46, 709-716.

Kajiwara, N., Noma, Y., Takigami, H., 2008. Photolysis studies of technical decabromodiphenyl ether (DecaBDE) and ethane (DeBDethane) in plastics under natural sunlight. Environ Sci Technol 42, 4404-4409.

Khaled, A., Richard, C., Redin, L., Niinipuu, M., Jansson, S., Jaber, F., Sleiman, M., 2018. Characterization and Photodegradation of Polybrominated Diphenyl Ethers in Car Seat Fabrics from End-of-Life Vehicles. Environ Sci Technol 52, 1216-1224.
Lin, C.S., Liu, W.L., Chiu, Y.S., Ho, S.-Y., 1992. Benzophenone-sensitized photodegradation of polystyrene films under atmospheric conditions. Polymer Degradation and Stability 38, 125-130.
Lin, u.W.L.W.P.F.Z.Z., 2015. Distribution of metals and brominated flame retardants (BFRs) in sediments, soils and plants from an informal e-waste dismantling site, South China. 22.
Liu, A., Shi, J., Qu, G., Hu, L., Ma, Q., Song, M., Jing, C., Jiang, G., 2017. Identification of Emerging Brominated Chemicals as the Transformation Products of Tetrabromobisphenol A (TBBPA) Derivatives in Soil. Environmental Science & Technology 51, 5434-5444.
Liu, Q., Ren, X., Long, Y., Hu, L., Qu, G., Zhou, Q., Jiang, G., 2016. The potential neurotoxicity of emerging tetrabromobisphenol A derivatives based on rat pheochromocytoma cells. Chemosphere 154, 194-203.
Morris, S., Allchin, C.R., Zegers, B.N., Haftka, J.J., Boon, J.P., Belpaire, C., Leonards, P.E., Van Leeuwen, S.P., De Boer, J., 2004. Distribution and fate of HBCD and TBBPA brominated flame retardants in North Sea estuaries and aquatic food webs. Environ Sci Technol 38, 5497-5504.
Pan, L., Bian, W., Zhang, J., 2013. The Effect of Explicit Solvent on Photodegradation of Decabromodiphenyl Ether in Toluene: Insights from Theoretical Study. The Journal of Physical Chemistry A 117, 5291-5298.
Qu, G., Liu, A., Wang, T., Zhang, C., Fu, J., Yu, M., Sun, J., Zhu, N., Li, Z., Wei, G., Du, Y., Shi, J., Liu, S., Jiang, G., 2013. Identification of tetrabromobisphenol A allyl ether and tetrabromobisphenol A 2,3-dibromopropyl ether in the ambient environment near a manufacturing site and in mollusks at a coastal region. Environ Sci Technol 47, 4760-4767.
Sindiku, O., Babayemi, J., Osibanjo, O., Schlummer, M., Schluep, M., Watson, A., Weber, R., 2015. Polybrominated diphenyl ethers listed as Stockholm Convention POPs, other brominated flame retardants and heavy metals in e-waste polymers in Nigeria. Environ Sci Pollut Res Int 22, 14489-14501.
Sinturel, C., Philippart, J.-L., Lemaire, J., Gardette, J.-L., 1999. Photooxidation of fire retarded polypropylene. I. Photoageing in accelerated conditions. European Polymer Journal 35, 1773-1781.
Staszowska, A.B., 2017. Photodegradation of lower polybrominated diphenyl ether congeners in indoor air - model studies. Journal of Ecological Engineering 18, 180-186.
Torikai, A., Kobatake, T., Okisaki, F., Shuyama, H., 1995. Photodegradation of polystyrene containing flame-retardants: wavelength sensitivity and efficiency of degradation. Polymer Degradation and Stability 50, 261-267.
Van der Ven, L.T., Van de Kuil, T., Verhoef, A., Verwer, C.M., Lilienthal, H., Leonards, P.E., Schauer, U.M., Canton, R.F., Litens, S., De Jong, F.H., Visser, T.J., Dekant, W., Stern, N., Hakansson, H., Slob, W., Van den Berg, M., Vos, J.G., Piersma, A.H., 2008. Endocrine effects of tetrabromobisphenol-A (TBBPA) in Wistar rats as tested in a one-generation reproduction study and a subacute toxicity study. Toxicology 245, 76-89.
Wang, M., Wang, H., Zhang, R., Ma, M., Mei, K., Fang, F., Wang, X., 2015a. Photolysis of Low-Brominated Diphenyl Ethers and Their Reactive Oxygen Species-Related Reaction Mechanisms in an Aqueous System. PLoS One 10, e0135400.
Wang, X., Hu, X., Zhang, H., Chang, F., Luo, Y., 2015b. Photolysis Kinetics, Mechanisms, and Pathways of Tetrabromobisphenol A in Water under Simulated Solar Light Irradiation. Environ Sci Technol 49, 6683-6690.
Zhang, Y.N., Chen, J., Xie, Q., Li, Y., Zhou, C., 2016. Photochemical transformation of five novel brominated flame retardants: Kinetics and photoproducts. Chemosphere 150, 453-460.

Highlights

- Quantum yields of four BFRs were measured in tetrahydrofuran and polystyrene
- Higher photoreactivity of BFRs was observed in polystyrene
- Photodegradation of BFRs induced oxidation and yellowing of polystyrene
- The less absorbing BFR was found to be further degraded during irradiation
- C7-brominated photoproducts of polystyrene oxidation were detected for the first time